

## Investigations on Synthesis, Structure, and Properties of New Butterfly [2Fe2Se] Cluster Complexes Relevant to Active Sites of Some Hydrogenases

Li-Cheng Song,\* Wei Gao, Cui-Ping Feng, De-Fu Wang, and Qing-Mei Hu

Department of Chemistry, State Key Laboratory of Elemento-Organic Chemistry, Nankai University, Tianjin 300071, People's Republic of China

Received July 3, 2009

As a continuation of our studies on biomimetic chemistry and butterfly cluster chemistry, two series of “closed” and “open” butterfly [2Fe2Se] cluster complexes have been prepared in satisfactory yields. Thus, treatment of  $\text{Fe}_3(\text{CO})_{12}$  with  $(\text{HSeCH}_2)_2\text{CHOH}$  in toluene at reflux gave the expected “closed” butterfly [2Fe2Se] cluster complex  $[(\mu\text{-SeCH}_2)_2\text{CH}(\text{OH})]\text{Fe}_2(\text{CO})_6$  (**A**), whereas the “open” butterfly cluster complex  $(\mu\text{-EtSe})[(\mu\text{-SeCH}_2\text{CH}(\text{OH})(\text{CH}_2\text{Br}))\text{Fe}_2(\text{CO})_6$  (**B**) was unexpectedly produced along with complex **A** via a sequential reaction of  $(\mu\text{-Se}_2)\text{Fe}_2(\text{CO})_6$  with  $\text{Et}_3\text{BHLi}$ , followed by treatment with  $(\text{BrCH}_2)_2\text{CHOH}$ . The other “closed” and “open” cluster complexes **1–6** could be further prepared by the hydroxy transformation and CO substitution reactions of complexes **A** and **B**. For example, (i) reaction of **A** with  $\text{PPh}_3$  and decarbonylating agent  $\text{Me}_3\text{NO}$  afforded  $\text{PPh}_3$ -monosubstituted complex  $[(\mu\text{-SeCH}_2)_2\text{CH}(\text{OH})]\text{Fe}_2(\text{CO})_5(\text{PPh}_3)$  (**1**), (ii) further reaction of **1** with the acylating agent  $\text{PhC}(\text{O})\text{Cl}$  in the presence of  $\text{Et}_3\text{N}$  produced the benzoate-functionalized complex  $[(\mu\text{-SeCH}_2)_2\text{CH}(\text{O}_2\text{CPh})]\text{Fe}_2(\text{CO})_5(\text{PPh}_3)$  (**2**), (iii) treatment of **A** with the phosphatizing agent  $\text{Ph}_2\text{PCl}$  in the presence of  $\text{Et}_3\text{N}$  or simply with  $\text{PhPCl}_2$  yielded the phosphite-functionalized complexes  $[(\mu\text{-SeCH}_2)_2\text{CH}(\text{OPPh}_2\text{-}\eta^1)]\text{Fe}_2(\text{CO})_5$  (**3**) and  $[(\mu\text{-SeCH}_2)_2\text{CH}(\text{OPPhCl-}\eta^1)]\text{Fe}_2(\text{CO})_5$  (**4**), and (iv) treatment of **B** with 4-pyridinecarboxylic chloride or  $\text{Ph}_2\text{PCl}$  in the presence of  $\text{Et}_3\text{N}$  resulted in formation of the “open” butterfly cluster complexes  $(\mu\text{-EtSe})[(\mu\text{-SeCH}_2\text{CH}(\text{CH}_2\text{Br})\text{-}(\text{O}_2\text{CC}_5\text{H}_4\text{N-4}))]\text{Fe}_2(\text{CO})_6$  (**5**) and  $(\mu\text{-EtSe})[(\mu\text{-SeCH}_2\text{CH}(\text{CH}_2\text{Br})(\text{OPPh}_2\text{-}\eta^1))]\text{Fe}_2(\text{CO})_5$  (**6**). All the new complexes have been characterized by elemental analysis and spectroscopy, as well as for **A**, **1–4**, and **6** by X-ray crystallography. Both  $^1\text{H}$  and  $^{77}\text{Se}$  NMR spectral studies demonstrated that complexes **B** and **5** consist of three isomers of e-Et/a-R, e-Et/e-R, and a-Et/e-R, whereas complex **6** exists only as one isomer of e-Et/a-R. On the basis of an electrochemical study, it was found that the “closed” and “open” complexes **A** and **B** can catalyze the proton reduction of TsOH and HOAc to give hydrogen, respectively.

### Introduction

The butterfly [2Fe2E] (E = S, Se) cluster complexes with general formula  $(\mu\text{-RE})_2\text{Fe}_2(\text{CO})_n\text{L}_{6-n}$  (L = 2e ligands) have recently attracted ever more attention because of their rich and varied chemistry<sup>1–3</sup> and particularly their close relationship with biomimetic chemistry of the natural enzymes of FeFe-hydrogenases (FeFeHases), NiFe-hydrogenases (NiFeHases),

and NiFeSe-hydrogenases (NiFeSeHases).<sup>4,5</sup> The three groups of hydrogenases are highly efficient enzymes, which can catalyze the reversible redox reaction between hydrogen and protons in various microorganisms.<sup>6</sup> Figure 1 compares their active site structures obtained from the corresponding enzyme

\*To whom correspondence should be addressed. Fax: 0086-22-23504853. E-mail: lcsong@nankai.edu.cn.

(1) (a) Seyferth, D.; Henderson, R. S.; Song, L.-C. *Organometallics* **1982**, *1*, 125. (b) Seyferth, D.; Womack, G. B.; Archer, C. M.; Dewan, J. C. *Organometallics* **1989**, *8*, 430. (c) Seyferth, D.; Ruschke, D. P.; Davis, W. M.; Cowie, M.; Hunter, A. D. *Organometallics* **1994**, *13*, 3834.

(2) (a) Song, L.-C. *Acc. Chem. Res.* **2005**, *38*, 21. (b) Song, L.-C. *Trends Organomet. Chem.* **1999**, *3*, 1. (c) Song, L.-C. *Sci. China Ser. B: Chem.* **2009**, *52*, 1.

(3) (a) Ogino, H.; Inomata, S.; Tobita, H. *Chem. Rev.* **1998**, *98*, 2093. (b) Hieber, W.; Gruber, J. Z. *Anorg. Allg. Chem.* **1958**, *296*, 91. (c) Mathur, P.; Manimaran, B.; Trivedi, R.; Hossain, M. M.; Arabatti, M. J. *Organomet. Chem.* **1996**, *515*, 155.

(4) (a) Darensbourg, M. Y.; Lyon, E. J.; Smee, J. J. *Coord. Chem. Rev.* **2000**, *206–207*, 533. (b) Frey, M. *ChemBioChem* **2002**, *3*, 153. (c) Evans, D. J.; Pickett, C. J. *Chem. Soc. Rev.* **2003**, *32*, 268. (d) Tard, C.; Pickett, C. J. *Chem. Rev.* **2009**, *109*, 2245.

(5) (a) Fontecilla-Camps, J. C.; Volbeda, A.; Cavazza, C.; Nicolet, Y. *Chem. Rev.* **2007**, *107*, 4273. (b) Parkin, A.; Goldet, G.; Cavazza, C.; Fontecilla-Camps, J. C.; Armstrong, F. A. J. *Am. Chem. Soc.* **2008**, *130*, 13410.

(6) (a) Vignais, P. M.; Billoud, B. *Chem. Rev.* **2007**, *107*, 4206. (b) Cammack, R. *Nature* **1999**, *397*, 214. (c) Adams, M. W. W.; Stiefel, E. I. *Science* **1998**, *282*, 1842.

(7) (a) Peters, J. W.; Lanzilotta, W. N.; Lemon, B. J.; Seefeldt, L. C. *Science* **1998**, *282*, 1853. (b) Nicolet, Y.; Piras, C.; Legrand, P.; Hatchikian, C. E.; Fontecilla-Camps, J. C. *Structure* **1999**, *7*, 13.

(8) Nicolet, Y.; de Lacey, A. L.; Vernède, X.; Fernandez, V. M.; Hatchikian, E. C.; Fontecilla-Camps, J. C. *J. Am. Chem. Soc.* **2001**, *123*, 1596.

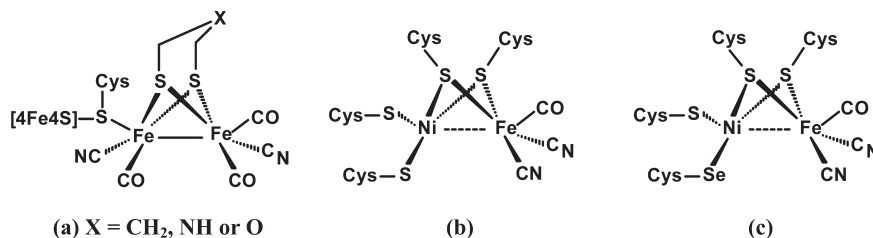
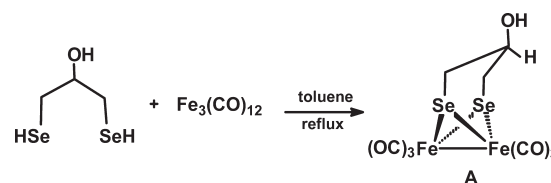


**Figure 1.** Comparison of the active site structures of (a) FeFeHases,<sup>7,8</sup> (b) NiFeHases,<sup>9</sup> and (c) NiFeSeHases.<sup>10</sup>

crystallographic studies.<sup>7–10</sup> As shown in Figure 1, the three active sites have the following structural features: (i) the active site for FeFeHases contains a butterfly [2Fe2S] cluster, whereas the NiFe- and NiFeSe-hydrogenases' active sites have a butterfly [NiFe2S] cluster, (ii) the two Fe atoms in the butterfly [2Fe2S] cluster and the Fe atom in the butterfly [NiFe2S] cluster are coordinated by CO and CN<sup>-</sup> ligands, whereas the bimetallic centers in these butterfly clusters are all bridged by thiolate ligands, (iii) whereas the thiolate ligands in FeFeHases are a dithiolate SCH<sub>2</sub>XCH<sub>2</sub>S, those of NiFeHases and NiFeSeHases are two CysS monothiolates (CysS = cysteinyl), and (iv) whereas one of the iron atoms in the butterfly [2Fe2S] cluster of FeFeHases is linked to a cubic [4Fe4S] cluster via the sulfur atom of CysS ligand, the nickel atom in NiFeHases is coordinated by two terminal CysS ligands and that in NiFeSeHases by one terminal CysS ligand and one terminal CysSe ligand, respectively.

In view of the interesting chemistry and the structural similarity of complexes ( $\mu$ -RE)<sub>2</sub>Fe<sub>2</sub>(CO)<sub>n</sub>L<sub>6-n</sub> with the above-mentioned enzyme active sites, we and others have

**Scheme 1**



prepared a great variety of such butterfly [2Fe2E] cluster complexes, many of which have been used as the active site models of FeFe-hydrogenases.<sup>11–14</sup> As part of our projects associated with the butterfly Fe/E cluster chemistry and biomimetic chemistry of hydrogenases, we report the synthesis, structural characterization, and properties of two series of butterfly [2Fe2Se] cluster complexes, which are closely related to the active sites of FeFe-, NiFe-, and NiFeSe-hydrogenases.

## Results and Discussion

**Synthesis and Characterization of [( $\mu$ -SeCH<sub>2</sub>)<sub>2</sub>CH(OH)]-Fe<sub>2</sub>(CO)<sub>6</sub> (A) and ( $\mu$ -EtSe)[( $\mu$ -SeCH<sub>2</sub>CH(OH)(CH<sub>2</sub>Br)]Fe<sub>2</sub>(CO)<sub>6</sub> (B).** The C-hydroxy-functionalized butterfly [2Fe2Se] cluster complex **A**, similar to its parent complex [ $\mu$ -Se(CH<sub>2</sub>)<sub>3</sub>Se- $\mu$ ]Fe<sub>2</sub>(CO)<sub>6</sub>,<sup>14b,14c</sup> could be prepared by oxidative addition of 1,3-dihydroseleto-2-propanol with Fe<sub>3</sub>(CO)<sub>12</sub> in toluene at reflux in 51% yield (Scheme 1).

Complex **A** is an air-stable red solid, which was fully characterized by elemental analysis, spectroscopy, and X-ray crystal diffraction analysis. The IR spectrum of **A** showed three absorption bands in the range 2068–1989 cm<sup>-1</sup> for its terminal carbonyls and one broad band centered at 3418 cm<sup>-1</sup> for its hydroxy group. The <sup>1</sup>H NMR spectrum of **A** displayed one doublet at 1.85 ppm for the hydrogen atom in its equatorial hydroxyl group (confirmed by X-ray crystallography, vide infra) and one triplet at 1.53 ppm and one doublet at 2.84 ppm for the axial and equatorial hydrogen atoms in its two CH<sub>2</sub> groups. The <sup>77</sup>Se NMR spectrum of **A** exhibited a singlet at 207.36 ppm for its two identical Se atoms bridged by a hydroxylpropylene group. This <sup>77</sup>Se NMR value is much larger than that of its parent complex (145.0 ppm<sup>14b</sup> and 150.6 ppm<sup>14c</sup>), owing to the presence of an electron-withdrawing hydroxy group in **A** and the <sup>77</sup>Se NMR data being highly sensitive to the Se coordination mode and the chemical environment around the Se atom.<sup>15</sup>

The molecular structure of **A** was unequivocally confirmed by X-ray crystallography. While Figure 2 shows its ORTEP drawing, selected bond lengths and angles are given

(9) (a) Volbeda, A.; Garcin, E.; Piras, C.; de Lacey, A. L.; Fernandez, V. M.; Hatchikian, E. C.; Frey, M.; Fontecilla-Camps, J. C. *J. Am. Chem. Soc.* **1996**, *118*, 12989. (b) Higuchi, Y.; Ogata, H.; Miki, K.; Yasuoka, N.; Yagi, T. *Structure* **1999**, *7*, 549.

(10) (a) Garcin, E.; Venede, X.; Hatchikian, E. C.; Volbeda, A.; Frey, M.; Fontecilla-Camps, J. C. *Structure* **1999**, *7*, 557. (b) Stein, M.; Lubitz, W. *Phys. Chem. Chem. Phys.* **2001**, *3*, 5115.

(11) (a) Gloaguen, F.; Lawrence, J. D.; Schmidt, M.; Wilson, S. R.; Rauchfuss, T. B. *J. Am. Chem. Soc.* **2001**, *123*, 12518. (b) Lyon, E. J.; Georgakaki, I. P.; Reibenspies, J. H.; Darensbourg, M. Y. *J. Am. Chem. Soc.* **2001**, *123*, 3268. (c) Razavet, M.; Davies, S. C.; Hughes, D. L.; Barclay, J. E.; Evans, D. J.; Fairhurst, S. A.; Liu, X.; Pickett, C. J. *Dalton Trans.* **2003**, 586. (d) Thomas, C. M.; Liu, T.; Hall, M. B.; Daresbourg, M. Y. *Inorg. Chem.* **2008**, *47*, 7009. (e) Song, L.-C.; Cheng, J.; Yan, J.; Wang, H.-T.; Liu, X.-F.; Hu, Q.-M. *Organometallics* **2006**, *25*, 1544. (f) Zhong, W.; Zampella, G.; Li, Z.; De Gioia, L.; Liu, Y.; Zeng, X.; Luo, Q.; Liu, X. *J. Organomet. Chem.* **2008**, *693*, 3751. (g) Li, P.; Wang, M.; He, C.; Li, G.; Liu, X.; Chen, C.; Åkermark, B.; Sun, L. *Eur. J. Inorg. Chem.* **2005**, 2506.

(12) (a) Lawrence, J. D.; Li, H.; Rauchfuss, T. B.; Bénard, M.; Rohmer, M.-M. *Angew. Chem., Int. Ed.* **2001**, *40*, 1768. (b) Li, H.; Rauchfuss, T. B. *J. Am. Chem. Soc.* **2002**, *124*, 726. (c) Capon, J.-F.; Ezzaher, S.; Gloaguen, F.; Pétilion, F. Y.; Schollhammer, P.; Talarmin, J. *Chem.—Eur. J.* **2008**, *14*, 1954. (d) Song, L.-C.; Tang, M.-Y.; Su, F.-H.; Hu, Q.-M. *Angew. Chem., Int. Ed.* **2006**, *45*, 1130. (e) Song, L.-C.; Tang, M.-Y.; Mei, S.-Z.; Huang, J.-H.; Hu, Q.-M. *Organometallics* **2007**, *26*, 1575. (f) Si, G.; Wang, W.-G.; Wang, H.-Y.; Tung, C.-H.; Wu, L.-Z. *Inorg. Chem.* **2008**, *47*, 8101.

(13) (a) Song, L.-C.; Yang, Z.-Y.; Bian, H.-Z.; Hu, Q.-M. *Organometallics* **2004**, *23*, 3082. (b) Song, L.-C.; Yang, Z.-Y.; Hua, Y.-J.; Wang, H.-T.; Liu, Y.; Hu, Q.-M. *Organometallics* **2007**, *26*, 2106. (c) Windhager, J.; Rudolph, M.; Bräutigam, S.; Görls, H.; Weigand, W. *Eur. J. Inorg. Chem.* **2007**, 2748.

(14) (a) Gao, S.; Fan, J.; Sun, S.; Peng, X.; Zhao, X.; Hou, J. *Dalton Trans.* **2008**, 2128. (b) Harb, M. K.; Niksch, T.; Windhager, J.; Görls, H.; Holze, R.; Lockett, L. T.; Okumura, N.; Evans, D. H.; Glass, R. S.; Lichtenberger, D. L.; El-khateeb, M.; Weigand, W. *Organometallics* **2009**, *28*, 1039. (c) Song, L.-C.; Gai, B.; Wang, H.-T.; Hu, Q.-M. *J. Inorg. Biochem.* **2009**, *103*, 805. (d) Harb, M. K.; Windhager, J.; Daraosheh, A.; Görls, H.; Lockett, L. T.; Okumura, N.; Evans, D. H.; Glass, R. S.; Lichtenberger, D. L.; El-khateeb, M.; Weigand, W. *Eur. J. Inorg. Chem.* **2009**, 3414.

(15) (a) Song, L.-C.; Yang, J.; Hu, Q.-M.; Wu, Q.-J. *Organometallics* **2001**, *20*, 3293. (b) van Hal, J. W.; Whitmire, K. H. *Organometallics* **1998**, *17*, 5197. (c) Luthra, N. P.; Boccanfuso, A. M.; Dunlap, R. B.; Odom, J. D. *J. Organomet. Chem.* **1988**, *354*, 51. (d) Wardle, R. W. M.; Mahler, C. H.; Chau, C.-N.; Ibers, J. A. *Inorg. Chem.* **1988**, *27*, 2790.

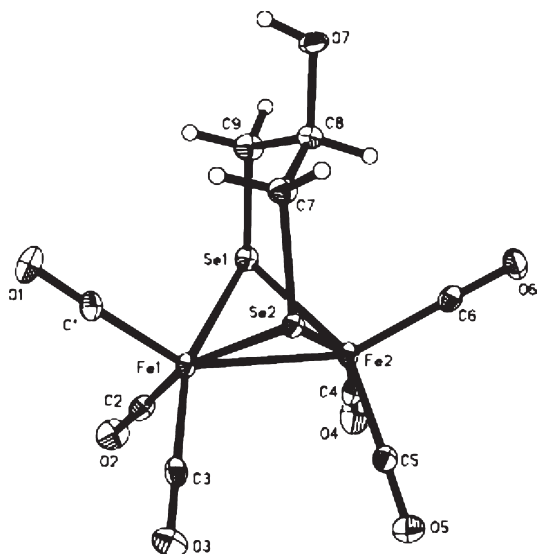


**Figure 2.** Molecular structure of **A** with 30% probability level ellipsoids.

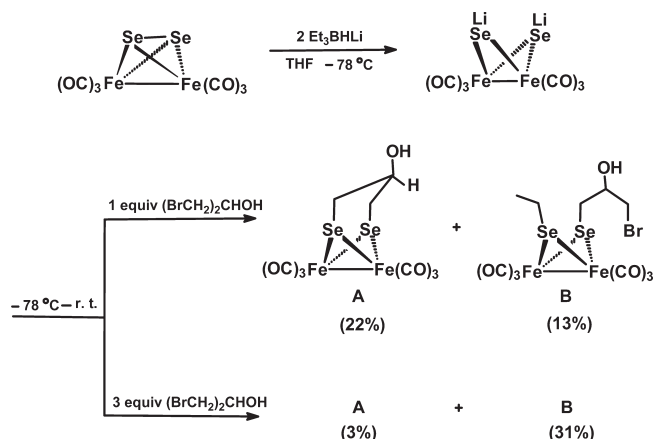
**Table 1.** Selected Bond Lengths (Å) and Angles (deg) for **A**, **1**, and **2**

A			
Se(1)–Fe(1)	2.3706(8)	Se(2)–C(7)	1.964(4)
Se(1)–Fe(2)	2.3714(8)	Fe(1)–Fe(2)	2.5598(9)
Se(2)–Fe(1)	2.3578(8)	C(7)–C(8)	1.501(6)
Se(2)–Fe(2)	2.3685(8)	O(7)–C(8)	1.434(5)
Fe(1)–Se(1)–Fe(2)	65.34(2)	Se(2)–Fe(1)–Fe(2)	57.41(2)
C(7)–Se(2)–Fe(1)	108.39(13)	Se(1)–Fe(1)–Fe(2)	57.34(2)
Fe(1)–Se(2)–Fe(2)	65.59(2)	Se(2)–Fe(2)–Se(1)	87.11(2)
Se(2)–Fe(1)–Se(1)	87.38(2)	C(7)–C(8)–C(9)	114.1(4)
1			
Se(1)–Fe(1)	2.3821(9)	Fe(2)–P(1)	2.2546(14)
Se(1)–Fe(2)	2.3774(7)	Fe(1)–Fe(2)	2.5777(11)
Se(2)–Fe(1)	2.3717(8)	C(6)–C(7)	1.504(5)
Se(2)–Fe(2)	2.3800(7)	O(6)–C(7)	1.445(4)
Fe(1)–Se(1)–Fe(2)	65.58(2)	P(1)–Fe(2)–Fe(1)	157.55(3)
Se(2)–Fe(1)–Fe(2)	57.30(3)	Se(1)–Fe(1)–Fe(2)	57.12(3)
Fe(1)–Se(2)–Fe(2)	65.70(3)	Se(2)–Fe(2)–Fe(1)	56.99(2)
Se(2)–Fe(1)–Se(1)	85.97(3)	C(6)–C(7)–C(8)	115.1(4)
2			
Se(1)–Fe(1)	2.4129(8)	Fe(1)–P(1)	2.2481(13)
Se(1)–Fe(2)	2.3827(8)	Fe(1)–Fe(2)	2.5509(9)
Se(2)–Fe(1)	2.3768(8)	C(11)–C(12)	1.507(6)
Se(2)–Fe(2)	2.3771(9)	O(11)–C(12)	1.467(5)
Fe(1)–Se(1)–Fe(2)	64.27(3)	P(1)–Fe(1)–Fe(2)	158.96(4)
Se(2)–Fe(1)–Fe(2)	57.55(2)	Se(1)–Fe(1)–Fe(2)	57.29(2)
Fe(1)–Se(2)–Fe(2)	64.90(3)	Se(2)–Fe(2)–Fe(1)	57.54(3)
Se(2)–Fe(1)–Se(1)	85.99(3)	C(11)–C(12)–C(13)	114.5(4)

in Table 1. Figure 2 shows that complex **A** contains a hydroxypropanediselenolate ligand, which is bridged between the Fe1 and Fe2 atoms to form a “closed” butterfly [2Fe2Se] cluster. The hydroxy group of **A** is indeed attached to atom C8 by a common equatorial bond of the chair and boat-like six-membered rings Fe1Se1C9C8C7Se2 and Fe2Se1C9C8C7Se2, whereas the hydrogen atom is connected to

(16) Song, L.-C.; Li, C.-G.; Gao, J.; Yin, B.-S.; Luo, X.; Zhang, X.-G.; Bao, H.-L.; Hu, Q.-M. *Inorg. Chem.* **2008**, *47*, 4545.

**Scheme 2**



C8 by the common axial bond. In fact, the structure of **A** is very similar to that of its sulfur analogue [( $\mu$ -SCH<sub>2</sub>)<sub>2</sub>CH(OH)]Fe<sub>2</sub>(CO)<sub>6</sub>.<sup>16</sup>

The “closed” complex **A** could also be prepared in 22% yield, along with 13% of complex **B**, by treatment of ( $\mu$ -LiSe)<sub>2</sub>Fe<sub>2</sub>(CO)<sub>6</sub> (generated in situ from ( $\mu$ -Se<sub>2</sub>)Fe<sub>2</sub>(CO)<sub>6</sub> and Et<sub>3</sub>BHLi)<sup>17</sup> with 1 equiv of 1,3-dibromo-2-propanol in THF from –78 °C to room temperature; however, further experiment showed that treatment of the in situ generated ( $\mu$ -LiSe)<sub>2</sub>Fe<sub>2</sub>(CO)<sub>6</sub> with an excess amount (3 equiv) of 1,3-dibromo-2-propanol under the same conditions resulted in formation of complex **B** as the major product along with a minor amount of **A** in 31% and 3% yields, respectively (Scheme 2).

Interestingly, the above-mentioned sequential reactions afforded two types of products (the expected “closed” **A** and the unexpected “open” product **B**) with different yields, mainly depending upon the molar ratio between intermediate ( $\mu$ -LiSe)<sub>2</sub>Fe<sub>2</sub>(CO)<sub>6</sub> and electrophile (BrCH<sub>2</sub>)<sub>2</sub>CHOH. In addition, the ethyl group in **B** most likely originates from Et<sub>3</sub>B that was released during the initial reductive cleavage reaction of the Se–Se bond of ( $\mu$ -Se<sub>2</sub>)Fe<sub>2</sub>(CO)<sub>6</sub> with Et<sub>3</sub>BHLi.<sup>17</sup> Although this is the first case in which an ethyl group of Et<sub>3</sub>B is transferred to the bridged Se atom of a butterfly [2Fe2Se] cluster, some cases are known in which an ethyl group of Et<sub>3</sub>B is transferred to the bridged S atom of a butterfly [2Fe2S] cluster in similar sequential reactions.<sup>18</sup>

While complex **A** was identified by comparison of its melting point and IR and <sup>1</sup>H NMR data with those of the same compound prepared above by oxidative addition method, complex **B** (an air-stable red liquid) was characterized by elemental analysis and IR, <sup>1</sup>H NMR, and <sup>77</sup>Se NMR spectroscopy. In principle, the “open” type of butterfly complex **B** may have three possible isomers: (i) e-Et/a-R, (ii) e-Et/e-R, and (iii) a-Et/e-R (R = CH<sub>2</sub>CH(OH)CH<sub>2</sub>Br), in which its two different substituents are connected to Se atoms of the butterfly [2Fe2Se] cluster core in equatorial/axial, equatorial/equatorial, or axial/equatorial positions (Figure 3); the axial/axial isomer for this type of complex could not exist due to the strong steric repulsions between the two substituents.<sup>1a,19</sup> Fortunately, the three isomers of **B**

(17) Seyferth, D.; Henderson, R. S. *J. Organomet. Chem.* **1980**, *204*, 333.

(18) Seyferth, D.; Song, L.-C.; Henderson, R. S. *J. Am. Chem. Soc.* **1981**, *103*, 5103.

(19) Shaver, A.; Fitzpatrick, P. J.; Steliou, K.; Butler, I. S. *J. Am. Chem. Soc.* **1979**, *101*, 1313.

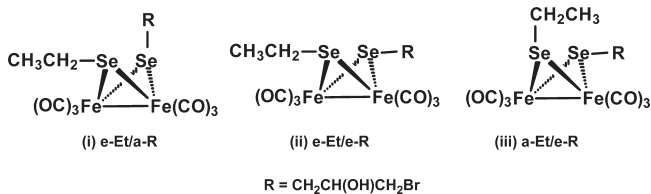


Figure 3. The three isomers of **B**.

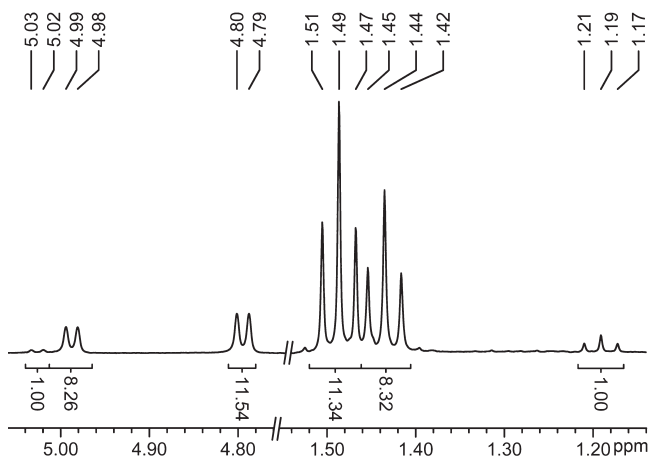


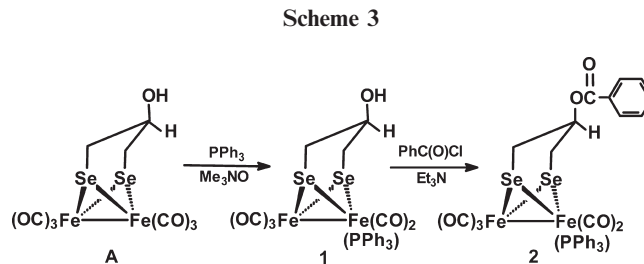
Figure 4. Partial  $^1\text{H}$  NMR spectrum of **B**.

have been proved by its  $^1\text{H}$  NMR spectrum (Figure 4), which shows three triplets at 1.49, 1.44, and 1.19 ppm and three doublets at 4.80, 4.99, and 5.03 ppm; these triplets and doublets could be reasonably assigned to the three different  $\text{CH}_3$  and OH groups in the equatorially and axially bound ethyl and  $\text{CH}_2\text{CH}(\text{OH})\text{CH}_2\text{Br}$  substituents in the three isomers. The isomer ratio was obtained as (i):(ii):(iii)  $\approx$  11:8:1 according to the integrated values of the corresponding three  $^1\text{H}$  NMR signals for the  $\text{CH}_3$  or OH group.

Interestingly, the  $^{77}\text{Se}$  NMR spectrum of **B** displayed six singlets in the range 95.72–206.96 ppm, consistent with the fact that **B** has six different Se atoms in its three isomers. In addition, the IR spectrum of **B** displayed three absorption bands in the region 2063–1980  $\text{cm}^{-1}$  and one absorption band at 3407  $\text{cm}^{-1}$ , consistent with **B** having terminal CO's and a hydroxy group, although its three isomers could not be distinguished by the IR spectrum.

**Synthesis and Characterization of  $[(\mu\text{-SeCH}_2)_2\text{CH}(\text{OH})]\text{Fe}_2(\text{CO})_5(\text{PPh}_3)$  (**1**) and  $[(\mu\text{-SeCH}_2)_2\text{CH}(\text{O}_2\text{CPh})]\text{Fe}_2(\text{CO})_5(\text{PPh}_3)$  (**2**).** We further found that butterfly  $[\text{2Fe}_2\text{Se}]$  cluster complexes **1** and **2** could be prepared by functional transformation reactions of the C-hydroxy and Fe-carbonyl functionalities of complex **A** with satisfactory yields. Thus, treatment of **A** with  $\text{PPh}_3$  and decarbonylating agent  $\text{Me}_3\text{NO}$ <sup>20</sup> in MeCN produced the  $\text{PPh}_3$ -monosubstituted complex **1** in 81% yield, whereas further reaction of **1** with benzoyl chloride in the presence of  $\text{Et}_3\text{N}$  in  $\text{CH}_2\text{Cl}_2$  afforded the corresponding benzoate-functionalized complex **2** in 76% yield (Scheme 3).

Complexes **1** and **2** are air-stable red solids, which were fully characterized by elemental analysis, spectroscopy, and X-ray crystallography. The IR spectra of **1** and **2** displayed three absorption bands in the region



2037–1928  $\text{cm}^{-1}$  for their terminal carbonyls, while **1** and **2** exhibited an additional band at 3387 or 1711  $\text{cm}^{-1}$  for their hydroxyl and ester carbonyl, respectively. Their highest  $\nu_{\text{C}=\text{O}}$  values, compared to that of complex **A**, are shifted by 33 and 36  $\text{cm}^{-1}$  toward lower energy. This is in accord with phosphine ligands being stronger  $\sigma$ -donors than CO.<sup>21</sup> The  $^1\text{H}$  NMR spectrum of **1** showed two doublets at 1.27 and 2.23 ppm for the axial and equatorial hydrogen atoms in its two  $\text{CH}_2\text{Se}$  groups, whereas complex **2** displayed a triplet at 1.52 ppm and a doublet at 2.47 ppm for the axial and equatorial hydrogen atoms in its two  $\text{CH}_2\text{Se}$  groups. In addition, the  $^{31}\text{P}$  NMR and  $^{77}\text{Se}$  NMR spectra of **1** and **2** exhibited a singlet at ca. 67 ppm and ca. 185 ppm for their  $\text{PPh}_3$  ligands and the two identical bridged Se atoms.

The molecular structures of **1** and **2** have also been confirmed by X-ray diffraction analysis (Figures 5, 6 and Table 1). Similarly, they contain a bridgehead C-hydroxyl or a C-benzoate-functionalized 1,3-propanediselenolate (PDS) ligand bridged between two iron atoms of the  $\text{Fe}(\text{CO})_3$  and  $\text{Fe}(\text{CO})_2(\text{PPh}_3)$  units. In **1** and **2**, both hydroxyl and benzoate substituents lie in an equatorial position and both  $\text{PPh}_3$  ligands are located in an apical position of the square-pyramidal Fe2 or Fe1 atom. The Fe1–Fe2, P1–Fe2, and P1–Fe1 bond lengths of **1** (2.5777 Å; 2.2546 Å) and **2** (2.5509 Å; 2.2481 Å) are close to the corresponding ones of the previously reported phosphine-substituted butterfly  $[\text{2Fe}_2\text{E}]$  (E = S, Se) cluster complexes.<sup>11g,23</sup>

**Synthesis and Characterization of  $[(\mu\text{-SeCH}_2)_2\text{CH}(\text{OPPh}_2\eta^1)]\text{Fe}_2(\text{CO})_5$  (**3**) and  $[(\mu\text{-SeCH}_2)_2\text{CH}(\text{OPPhCl}\eta^1)]\text{Fe}_2(\text{CO})_5$  (**4**).** More interestingly, the phosphite-functionalized complexes **3** and **4**, in which their P atoms are coordinated to one Fe atom of the diiron subsite, were also prepared by functional transformation reactions of the C-hydroxy and Fe-carbonyl functionalities of complex **A**. Thus, treatment of complex **A** with  $\text{Ph}_2\text{P}(\text{Cl})$  in the presence of  $\text{Et}_3\text{N}$  in THF or simply with  $\text{PhPCl}_2$  in MeCN gave rise to complexes **3** and **4** in 78% and 69% yields, respectively (Scheme 4). It is evident that these two reactions involve the initially formed intermediates **M**<sub>1</sub> and **M**<sub>2</sub> by intermolecular condensation of **A** with phosphine chlorides, followed by intramolecular CO substitution of **M**<sub>1</sub> and **M**<sub>2</sub> by their P atoms.<sup>16</sup>

(21) (a) Song, L.-C.; Yang, Z.-Y.; Bian, H.-Z.; Liu, Y.; Wang, H.-T.; Liu, X.-F.; Hu, Q.-M. *Organometallics* **2005**, *24*, 6126. (b) Song, L.-C.; Li, C.-G.; Ge, J.-H.; Yang, Z.-Y.; Wang, H.-T.; Zhang, J.; Hu, Q.-M. *J. Inorg. Biochem.* **2008**, *102*, 1973. (c) Adam, F. I.; Hogarth, G.; Richards, I.; Sanchez, B. E. *Dalton Trans.* **2007**, 2495. (d) Collman, J. P.; Hegedus, L. S. *Principles and Applications of Organotransition Metal Chemistry*; University Science Books: Mill Valley, 1980; pp 81–89.

(22) Song, L.-C.; Ge, J.-H.; Zhang, X.-G.; Liu, Y.; Hu, Q.-M. *Eur. J. Inorg. Chem.* **2006**, 3204.

(23) Song, L.-C.; Wang, H.-T.; Ge, J.-H.; Mei, S.-Z.; Gao, J.; Wang, L.-X.; Gai, B.; Zhao, L.-Q.; Yan, J.; Wang, Y.-Z. *Organometallics* **2008**, *27*, 1409.

(20) (a) Albers, M. O.; Coville, N. J. *Coord. Chem. Rev.* **1984**, *53*, 227. (b) Shen, J.-K.; Gao, Y.-C.; Shi, Q.-Z.; Basolo, F. *Coord. Chem. Rev.* **1993**, *128*, 69.

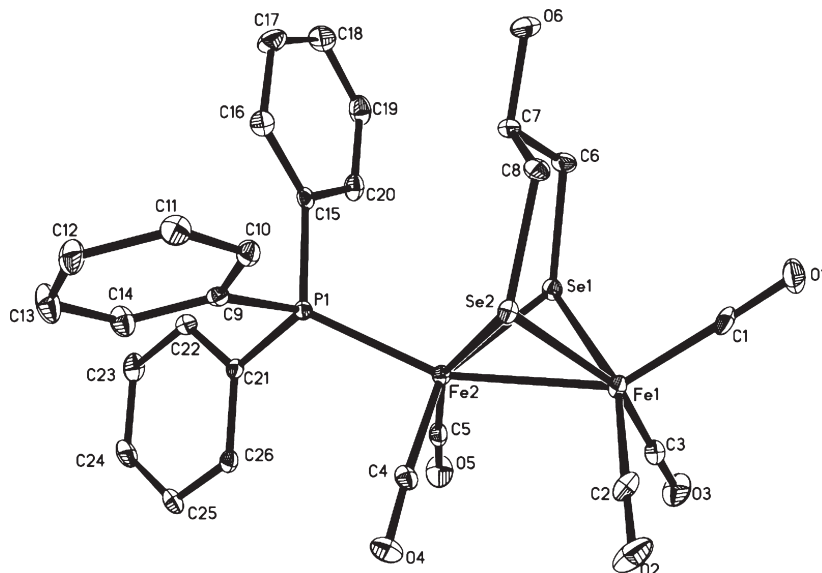


**Figure 5.** Molecular structure of **1** with 30% probability level ellipsoids.

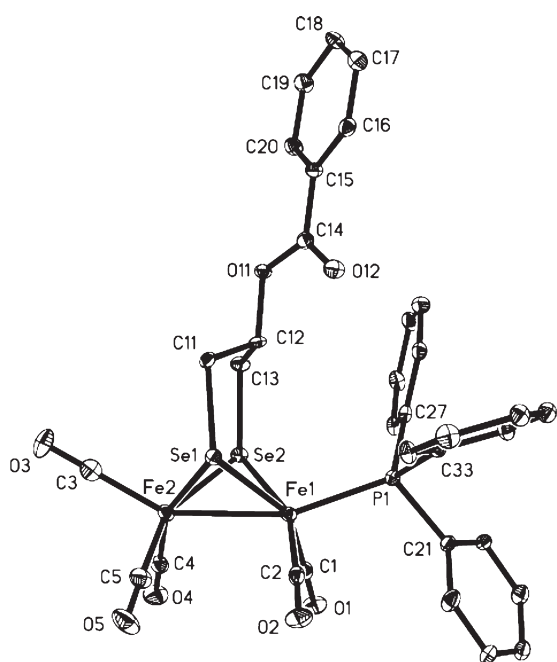
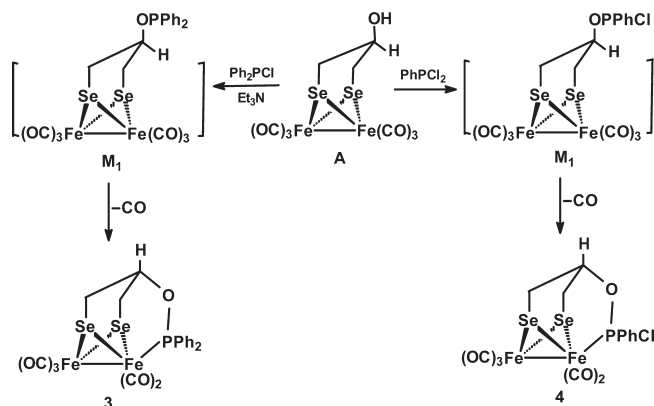


**Figure 6.** Molecular structure of **2** with 30% probability level ellipsoids.

Similar to **1** and **2**, complexes **3** and **4** are also air-stable red solids, which were characterized by elemental analysis and spectroscopy. The IR spectra of **3** and **4** displayed four absorption bands in the range 2043–1925  $\text{cm}^{-1}$  for their terminal carbonyls. The  $^{31}\text{P}$  NMR spectra exhibited a singlet at 159.47 and 207.66 ppm for their P atoms coordinated to the Fe atom in each diiron subsite. Particularly noteworthy is that the  $^1\text{H}$  NMR spectrum of **3** is quite different from that of **4**. For instance, complex **3** displayed two doublets at 1.97 and 2.60 ppm for its two axial  $\text{H}_a$  atoms and two equatorial  $\text{H}_c$  atoms, whereas **4** showed four doublets at 1.95, 2.15, 2.54, and 2.95 ppm for its two axial  $\text{H}_a$  and two equatorial  $\text{H}_c$  atoms (Figure 7). Why they displayed such different  $^1\text{H}$  NMR spectra is because the two  $\text{H}_a$  atoms or two  $\text{H}_c$  atoms in complex **3** are identical (with respect to the plane passing

**Scheme 4**



through its P atom, the central C atom of its diselenolate ligand, and the midpoint of its Fe–Fe bond) due to its P atom bearing two identical phenyl groups, but in complex **4** they are different due to the presence of an asymmetric P center with two different (Ph and Cl) groups. The  $^{77}\text{Se}$  NMR spectrum of **3** displayed only one singlet at 4.35 ppm for its two identical Se atoms, and **4** showed two singlets at 10.98 and 43.03 ppm for its two different Se atoms, which is consistent with the aforementioned different  $^1\text{H}$  NMR spectra of **3** and **4**.

The molecular structures of **3** and **4** have been unambiguously confirmed by X-ray diffraction analysis. Their ORTEP drawings are shown in Figures 8 and 9, whereas selected bond lengths and angles are listed in Table 2. Figures 8 and 9 indicate that complexes **3** and **4** contain a novel pentadentate ligand,  $(\mu\text{-SeCH}_2)_2\text{CH}(\text{OPPh}_2)\text{-}\eta^1$  or  $(\mu\text{-SeCH}_2)_2\text{CH}(\text{OPPhCl})\text{-}\eta^1$ , which is bridged between the two Fe atoms of  $\text{Fe}(\text{CO})_3$  and  $\text{Fe}(\text{CO})_2$  units to form the three fused six-membered rings  $\text{Fe1Se1C6C7C8Se2}$ ,  $\text{Fe2Se1C6C7C8Se2}$ , and  $\text{Fe2Se1C6C7O6P1}$ . The hydrogen atoms attached to their C7 atoms are, in contrast to the corresponding ones of complexes **A**, **1**, and **2**, lying in an equatorial position of the former two six-membered rings due to formation of the latter P-containing six-membered ring. Indeed, complex **3** is symmetric with respect to the plane passing through P1, C7,

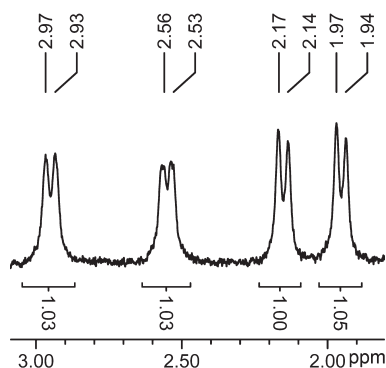


**Figure 7.**  $^1\text{H}$  NMR spectrum of the two  $\text{CH}_2\text{Se}$  groups in **4**.

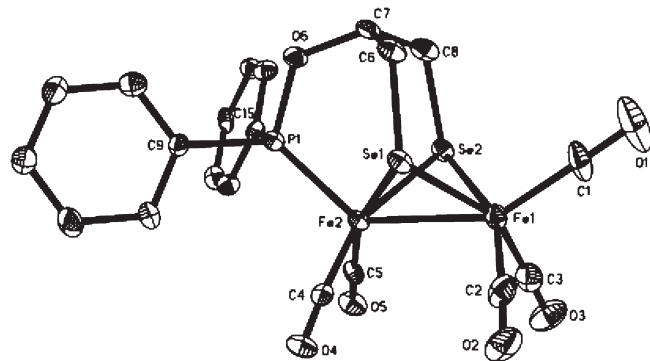


**Figure 8.** Molecular structure of **3** with 30% probability level ellipsoids.

and the midpoint of the  $\text{Fe1}-\text{Fe2}$  bond, while complex **4** is not symmetric with respect to the plane due to the P1 atom being attached to two different groups. Actually, the molecular crystal structures of **3** and **4** are in good agreement with their IR,  $^1\text{H}$  NMR, and  $^{77}\text{Se}$  NMR data, and they much resemble those of their sulfur analogues.<sup>16</sup>

**Synthesis and Characterization of  $(\mu\text{-EtSe})[\mu\text{-SeCH}_2\text{CH}(\text{CH}_2\text{Br})(\text{O}_2\text{CC}_5\text{H}_4\text{N-4})]\text{Fe}_2(\text{CO})_6$  (**5**) and  $(\mu\text{-EtSe})[\mu\text{-SeCH}_2\text{CH}(\text{CH}_2\text{Br})(\text{OPPh}_2\text{-}\eta^1)]\text{Fe}_2(\text{CO})_5$  (**6**).** The “open” butterfly  $[\text{2Fe}_2\text{Se}]$  cluster complexes **5** and **6** could be similarly prepared by functional transformation reactions of the C-hydroxy and Fe-carbonyl functionalities of the starting “open” complex **B**. Thus, treatment of complex **B** in  $\text{CH}_2\text{Cl}_2$  with 4-pyridinecarboxylic acid chloride in the presence of  $\text{Et}_3\text{N}$  gave the corresponding carboxylate-functionalized complex **5** in nearly quantitative yield, whereas complex **B** was treated in THF with  $\text{Ph}_2\text{PCl}$  and  $\text{Et}_3\text{N}$ , via intermediate **M**<sub>3</sub>, to afford the corresponding phosphite-functionalized complex **6** in 40% yield (Scheme 5).

While complex **5** is an air-stable red liquid, complex **6** is an air-stable red solid. Both complexes were characterized by elemental analysis and spectroscopy, and particularly for **6** by X-ray crystal diffraction analysis. The IR spectra of **5** and **6** showed three and four absorption bands in the range  $2064\text{--}1919\text{ cm}^{-1}$  for their terminal carbonyls, whereas **5** displayed an additional band at  $1737\text{ cm}^{-1}$  for its ester carbonyl. It is interesting to note that complex **5**, like its starting complex **B**, contains three isomers, (i) e-Et/a-R, (ii) e-Et/e-R, and (iii) a-Et/e-R ( $\text{R} = \text{CH}_2\text{CH}(\text{CH}_2\text{Br})\text{O}_2\text{CC}_5\text{H}_4\text{N-4}$ ), whereas complex **6** has only one isomer, namely, e-Et/a-R ( $\text{R} = \text{CH}_2\text{CH}(\text{CH}_2\text{Br})\text{OPPh}_2\text{-}\eta^1$ ). This is because the  $^1\text{H}$  NMR spectrum of **5** showed three triplets at 1.45, 1.38, and 1.13 ppm that could be assigned to the three different  $\text{CH}_3$  in

**Table 2.** Selected Bond Lengths ( $\text{\AA}$ ) and Angles (deg) for **3**, **4**, and **6**

<b>3</b>			
$\text{Fe(1)-Se(2)}$	2.3788(14)	$\text{Se(2)-C(8)}$	1.985(9)
$\text{Fe(1)-Se(1)}$	2.3858(15)	$\text{P(1)-O(6)}$	1.633(5)
$\text{Fe(2)-Se(2)}$	2.3627(12)	$\text{Fe(1)-Fe(2)}$	2.5385(17)
$\text{Fe(2)-Se(1)}$	2.3752(14)	$\text{Fe(2)-P(1)}$	2.192(2)
$\text{Se(2)-Fe(1)-Se(1)}$	87.67(5)	$\text{Fe(2)-Se(2)-Fe(1)}$	64.74(4)
$\text{Se(2)-Fe(1)-Fe(2)}$	57.32(4)	$\text{P(1)-Fe(2)-Fe(1)}$	135.92(7)
$\text{Se(1)-Fe(1)-Fe(2)}$	57.58(4)	$\text{Se(2)-Fe(2)-Fe(1)}$	57.94(4)
$\text{Se(2)-Fe(2)-Se(1)}$	88.29(4)	$\text{Se(1)-Fe(2)-Fe(1)}$	57.98(5)
<b>4</b>			
$\text{Se(1)-C(6)}$	1.963(3)	$\text{Fe(2)-P(1)}$	2.1469(11)
$\text{Se(1)-Fe(2)}$	2.3664(8)	$\text{Se(2)-Fe(2)}$	2.3653(8)
$\text{Se(1)-Fe(1)}$	2.3714(8)	$\text{Se(2)-Fe(1)}$	2.3752(8)
$\text{P(1)-O(6)}$	1.600(3)	$\text{Fe(1)-Fe(2)}$	2.5798(10)
$\text{Fe(2)-Se(1)-Fe(1)}$	65.98(3)	$\text{Se(2)-Fe(2)-Fe(1)}$	57.21(2)
$\text{Fe(2)-Se(2)-Fe(1)}$	65.94(3)	$\text{Se(1)-Fe(2)-Fe(1)}$	57.10(3)
$\text{Se(1)-Fe(1)-Se(2)}$	87.84(4)	$\text{Se(2)-Fe(1)-Fe(2)}$	56.84(3)
$\text{Se(1)-Fe(1)-Fe(2)}$	56.91(2)	$\text{P(1)-Fe(2)-Se(2)}$	90.15(4)
<b>6</b>			
$\text{Fe(1)-Se(2)}$	2.3729(11)	$\text{P(1)-C(17)}$	1.821(5)
$\text{Fe(1)-Se(1)}$	2.3822(10)	$\text{Fe(2)-Se(1)}$	2.3744(11)
$\text{Fe(1)-Fe(2)}$	2.5647(14)	$\text{Fe(2)-Se(2)}$	2.3851(13)
$\text{Fe(2)-P(1)}$	2.1865(14)	$\text{Br(1)-C(8)}$	1.939(5)
$\text{Se(2)-Fe(1)-Se(1)}$	83.43(3)	$\text{Se(1)-Fe(2)-Fe(1)}$	57.52(3)
$\text{Se(2)-Fe(1)-Fe(2)}$	57.61(4)	$\text{Se(2)-Fe(2)-Fe(1)}$	57.15(3)
$\text{Se(1)-Fe(1)-Fe(2)}$	57.22(3)	$\text{Fe(1)-Se(2)-Fe(2)}$	65.24(3)
$\text{P(1)-Fe(2)-Se(1)}$	93.73(5)	$\text{Fe(2)-Se(1)-Fe(1)}$	65.26(4)

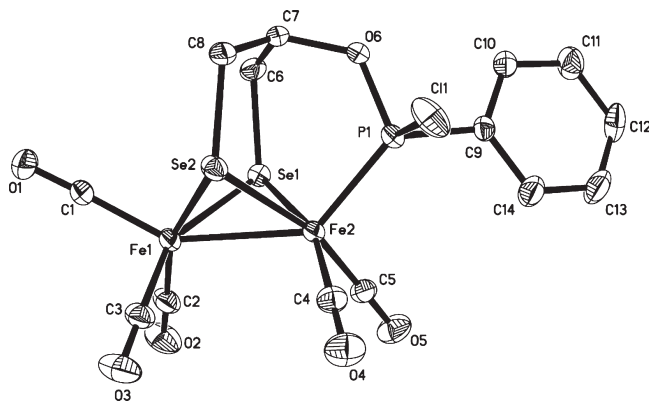


**Figure 9.** Molecular structure of **4** with 30% probability level ellipsoids.

the three equatorial and axial ethyl group-containing isomers; in addition, **6** displayed only one triplet at 0.96 ppm that was reasonably attributed to the  $\text{CH}_3$  in the equatorial ethyl group-containing isomer mentioned above. It follows that the  $^1\text{H}$  NMR spectra of **5** and **6** are consistent with the  $^{77}\text{Se}$  NMR spectrum of **5**, showing six singlets for its six different Se atoms in its three isomers, and that of **6**, showing two singlets for its two different Se atoms in its isomer e-Et/a- $\text{CH}_2\text{CH}(\text{CH}_2\text{Br})\text{OPPh}_2\text{-}\eta^1$ . Fortunately, the X-ray crystallographic study has unequivocally confirmed the molecular structure of complex **6**. The ORTEP plot of **6** is depicted in Figure 10. Table 2 lists selected bond lengths and angles. As shown intuitively in Figure 9, complex **6** consists of an open  $[\text{2Fe}_2\text{Se}]$  cluster core with five terminal carbonyls. The ethyl group is indeed equatorially attached to the Se2 atom through the C9-Se2 bond, while the phosphite ligand is

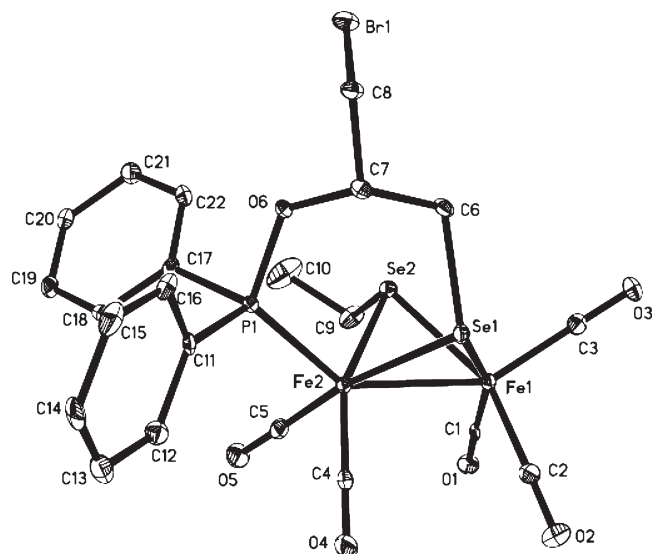
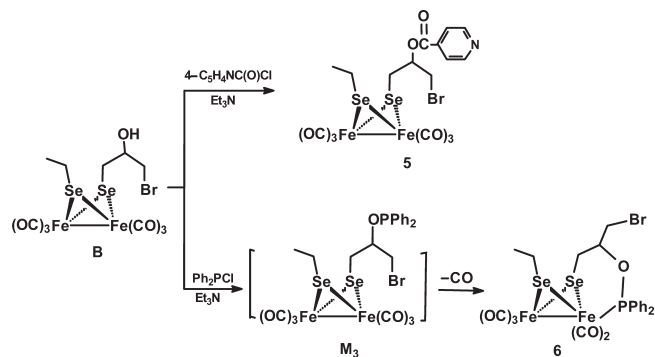


**Figure 10.** Molecular structure of **6** with 30% probability level ellipsoids.

### Scheme 5



axially connected to the Se1 atom via the C6–Se1 bond and apically coordinated to the Fe2 atom to form the six-membered P1Fe2Se1C6C7O6 metallaheterocycle. Although **6** is an “open” butterfly [2Fe2Se] cluster complex, its Fe1–Fe2 bond length (2.5647 Å) is very close to the corresponding ones for “closed” complexes **A** and **1–4** and the corresponding ones reported for the “closed” and “open” butterfly [2Fe2E] (E = S, Se) cluster complexes.<sup>14c,16,24</sup>

**Electrochemistry of A and B.** The electrochemical behavior of the representative models **A** and **B** were studied in MeCN under CO by cyclic voltammetric techniques. Table 3 lists their electrochemical data, and Figure 11 displays their cyclic voltammograms, respectively. It is shown that **A** exhibits one quasi-reversible reduction, one irreversible reduction, and one irreversible oxidation, whereas **B** displays two irreversible reductions and one irreversible oxidation. The first and second reduction peaks of **A** (−1.63 and −2.30 V) and **B** (−1.58 and −2.22 V) could be assigned to the one-electron reduction processes from Fe<sup>I</sup>Fe<sup>I</sup> to Fe<sup>I</sup>Fe<sup>0</sup> and Fe<sup>I</sup>Fe<sup>0</sup> to Fe<sup>0</sup>Fe<sup>0</sup> (supported by the calculated values of 1.11 and 1.09 Faraday/equiv obtained by study of the bulk electrolysis of a MeCN solution of **A** at −1.80 V and **B** at −1.77 V,<sup>25</sup>

**Table 3. Electrochemical Data of A, B, and C<sup>a</sup>**

compound	$E_{pc}, E_{pa}$ (V)	$E_{pc}$ (V)	$E_{pa}$ (V)
	Fe <sup>I</sup> Fe <sup>I</sup> /Fe <sup>I</sup> Fe <sup>0</sup>	Fe <sup>I</sup> Fe <sup>0</sup> /Fe <sup>0</sup> Fe <sup>0</sup>	Fe <sup>I</sup> Fe <sup>I</sup> /Fe <sup>I</sup> Fe <sup>II</sup>
<b>A</b>	−1.63, −1.53	−2.30	+0.70
<b>B</b>	−1.58, −	−2.22	+0.61
<b>C</b>	−1.61, −1.51	−2.16	+0.76

<sup>a</sup> All potentials are versus Fc/Fc<sup>+</sup> in 0.1 M *n*-Bu<sub>4</sub>NPF<sub>6</sub>/MeCN.

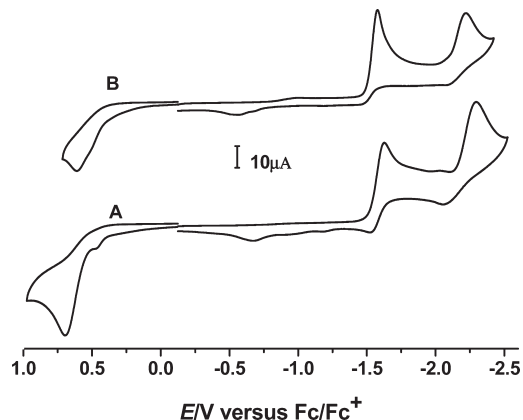


**Figure 11.** Cyclic voltammograms of **A** and **B** (1 mM) in 0.1 M *n*-Bu<sub>4</sub>NPF<sub>6</sub>/MeCN under CO at a scan rate of 100 mV s<sup>−1</sup>.

respectively). Similarly, the oxidation peaks of **A** (+0.70 V) and **B** (+0.61 V) should be attributed to the one-electron oxidation processes from Fe<sup>I</sup>Fe<sup>I</sup> to Fe<sup>I</sup>Fe<sup>II</sup>. To compare the CV behavior of **A** with its sulfur analogue [(μ-SCH<sub>2</sub>)<sub>2</sub>CH<sub>2</sub>-(OH)]Fe<sub>2</sub>(CO)<sub>6</sub> (**C**),<sup>16</sup> we determined the cyclic voltammogram of **C** (see Figure 11\* in the Supporting Information). As can be seen in Table 3 and Figure 11\*, complex **C** displays one quasi-reversible reduction peak at −1.61 V, one irreversible reduction peak at −2.16 V, and one irreversible oxidation peak at +0.76 V. Therefore, the CV behavior of **A** is very similar to that of **C**.

The cyclic voltammograms of **A** and **B** in the presence of *p*-toluenesulfonic acid (TsOH, p*K*<sub>a</sub> = 8.7 in MeCN) and acetic acid (HOAc, p*K*<sub>a</sub> = 22.3 in MeCN)<sup>26</sup> are presented in Figures 12 and 13, respectively. For comparison, the cyclic voltammograms of **A** and **B** without TsOH and HOAc are also included. It is shown that when the first 2 mM TsOH was added, the first reduction peak of **A** at −1.60 V obviously increased and continuously increased linearly with an increase in acid concentration. However, in contrast to this, when the first 2 mM HOAc was added, the first reduction peak of **B** at −1.57 V did not grow, but its second reduction peak at −2.24 V grew remarkably with increasing acid concentration. The rapid increase in current height of the reduction peak reveals an electrocatalytic processes.<sup>27–30</sup>

To further confirm the catalytic ability of **A** and **B** for H<sub>2</sub> production, a solution of **A** or **B** (0.5 mM) with an excess

(26) Izutsu, K. *Acid-Base Dissociation Constants in Dipolar Aprotic Solvents*; Blackwell Scientific Publications: Oxford, 1990.

(27) Bhugun, I.; Lexa, D.; Savéant, J.-M. *J. Am. Chem. Soc.* **1996**, *118*, 3982.

(28) Gloaguen, F.; Lawrence, J. D.; Rauchfuss, T. B. *J. Am. Chem. Soc.* **2001**, *123*, 9476.

(29) Chong, D.; Georgakaki, I. P.; Mejia-Rodriguez, R.; Sanabria-Chinchilla, J.; Soriaga, M. P.; Darensbourg, M. Y. *Dalton Trans.* **2003**, 4158.

(30) Borg, S. J.; Behrsing, T.; Best, S. P.; Razavet, M.; Liu, X.; Pickett, C. J. *J. Am. Chem. Soc.* **2004**, *126*, 16988.

(24) Song, L.-C.; Hu, Q.-M.; Wang, J.-T.; Lin, X.-Y.; Zheng, Q.-T.; Zhang, S.-D.; Shen, F.-L.; Wu, S. *Acta Chim. Sin.* **1986**, *44*, 558.

(25) Zanello, P. *Inorganic Electrochemistry Theory, Practice and Application*; Thomas Graham House: Cambridge, UK, 2003.

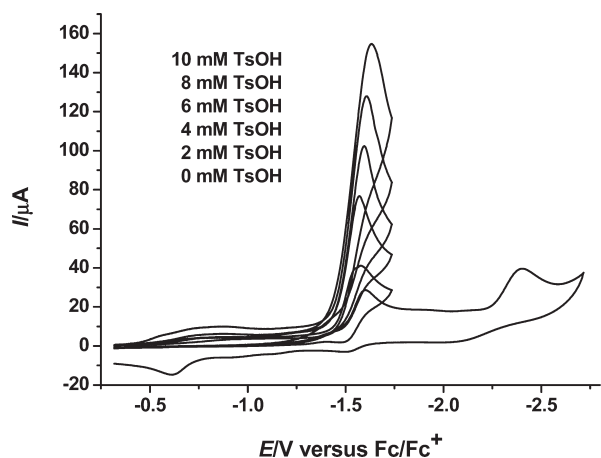


**Figure 12.** Cyclic voltammogram of **A** (1 mM) with TsOH (0–10 mM) in 0.1 M *n*-Bu<sub>4</sub>NPF<sub>6</sub>/MeCN under CO at a scan rate of 100 mV s<sup>-1</sup>.

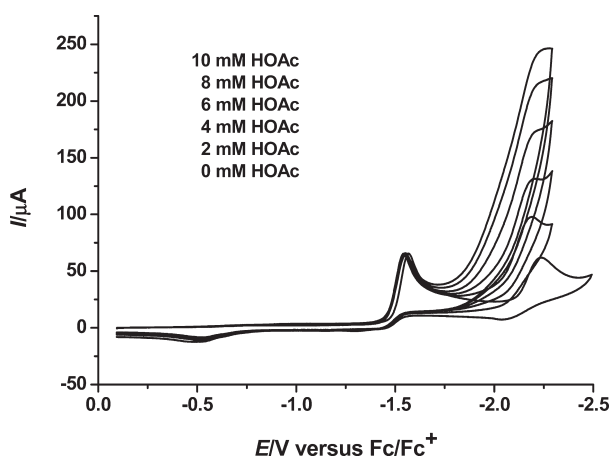


**Figure 13.** Cyclic voltammograms of **B** (1 mM) with TsOH (0–10 mM) in 0.1 M *n*-Bu<sub>4</sub>NPF<sub>6</sub>/MeCN under CO at a scan rate of 100 mV s<sup>-1</sup>.

amount of TsOH or HOAc (25 mM) was electrolyzed at  $-1.65$  and  $-2.34$  V, respectively. During 0.5 h electrolysis of TsOH, a total of 25.6 F per mole of **A** passed, which corresponds to 13 turnovers. Gas chromatographic analysis showed that the hydrogen yield was about 80%. Similarly, during 0.5 h electrolysis of HOAc, a total of 28.0 F per mole of **B** passed (which corresponds to 14 turnovers) and the hydrogen yield was about 90%.

Finally, it is worth pointing out that although numerous butterfly [2Fe2S] cluster-based model compounds were previously reported to have the catalytic ability for proton reduction to hydrogen,<sup>28–32</sup> very few butterfly [2Fe2Se] cluster complexes have been found to have such electrocatalytic behavior.<sup>14</sup>

## Conclusion

We have prepared the “closed” and “open” butterfly [2Fe2Se] cluster complexes, **A** and **B**, by oxidative addi-

tion of Fe<sub>3</sub>(CO)<sub>12</sub> with (HSeCH<sub>2</sub>)<sub>2</sub>CHOH and a sequential reaction of ( $\mu$ -Se<sub>2</sub>)Fe<sub>2</sub>(CO)<sub>6</sub> with Et<sub>3</sub>BHLi followed by treatment with (BrCH<sub>2</sub>)<sub>2</sub>CHOH, respectively. Further functional hydroxy transformation and CO substitution reactions of **A** and **B** have resulted in formation of the corresponding butterfly cluster complexes **1–6** with various functionalities. All these “closed” and “open” cluster complexes are new and have been fully characterized. Particularly noteworthy is that the molecular structures of solid complexes **A**, **1–4**, and **6** have been confirmed by X-ray crystal diffraction analysis, while liquid compound **B** and its derivative **5** have been established to exist as three isomers e-Et/a-R, e-Et/e-R, and a-Et/e-R by their <sup>1</sup>H and <sup>77</sup>Se NMR spectroscopic analysis. In view of the structural similarity of these “closed” and “open” cluster complexes with the active sites of FeFeHases, NiFeHases, and NiFeSeHases (although the “closed” complexes have more similarity with the active site of FeFeHases), we regarded these butterfly complexes as the active site models for these natural enzymes. In addition, we have demonstrated that the representative “closed” and “open” complexes **A** and **B** have the ability to catalyze the proton reduction of TsOH and HOAc to give hydrogen, respectively.

## Experimental Section

**General Comments.** While all reactions were performed using standard Schlenk and vacuum-line techniques under N<sub>2</sub>, all manipulations should be carried out in a well-ventilated hood, since all selenium-containing compounds are usually highly toxic. Toluene and THF were distilled from sodium/benzophenone ketyl, while MeCN and CH<sub>2</sub>Cl<sub>2</sub> were distilled from CaH<sub>2</sub>. Fe<sub>3</sub>(CO)<sub>12</sub>,<sup>33</sup> PhPCl<sub>2</sub>,<sup>34</sup> ( $\mu$ -Se<sub>2</sub>)Fe<sub>2</sub>(CO)<sub>6</sub>,<sup>17</sup> and 4-pyridinecarboxylic acid chloride<sup>35</sup> were prepared according to the published methods. Selenium powders, NaBH<sub>4</sub>, 1,3-dibromo-2-propanol (85%), Ph<sub>2</sub>PCl, Et<sub>3</sub>BHLi (1 M in THF), and other chemicals were purchased from commercial suppliers and used as received. Preparative TLC was carried out on glass plates (25 × 15 × 0.25 cm coated with silica gel G (10–40  $\mu$ m)). IR spectra were recorded on a Bio-Rad FTS 135 infrared spectrophotometer. <sup>1</sup>H (<sup>31</sup>P, <sup>77</sup>Se) NMR spectra were taken on a Bruker Avance 300 NMR, a Varian Mercury 300 NMR or a Varian Mercury Plus 400 NMR spectrometer, respectively. Elemental analyses were performed with an Elementar Vario EL analyzer. Melting points were determined on a Yanaco MP-500 apparatus and were uncorrected.

**Preparation of (HSeCH<sub>2</sub>)<sub>2</sub>CHOH.** This hydroxydiselenol was recently prepared by a complicated method.<sup>36</sup> However, we could prepare it by a simple and convenient method. A stirred suspension of selenium powders (0.790 g, 10.0 mmol) in absolute ethanol (20 mL) was cooled to 0 °C, and then NaBH<sub>4</sub> (0.390 g, 10.0 mmol) was slowly added. The mixture was stirred at 0 °C for an additional 0.5 h to give a solution containing sodium hydrogenselenide.<sup>37</sup> To this solution was added 1,3-dibromo-2-propanol (0.48 mL, 5.0 mmol), and then the new mixture was warmed to room temperature and stirred at this temperature for 3.5 h. After addition of the degassed water (20 mL), a given amount of dilute hydrochloric acid was added in order to lower the pH value of the mixture to 1–2. The H<sub>2</sub>Se present in the mixture was completely removed by bubbling nitrogen in a well-

(33) King, R. B. *Organometallic Syntheses; Transition-Metal Compounds*; Academic Press: New York, 1965; Vol. 1, p 95.

(34) Pass, F.; Schindlbauer, H. *Monatsh. Chem.* **1959**, *90*, 148.

(35) Meyers, A. I.; Gabel, R. A. *J. Org. Chem.* **1982**, *47*, 2633.

(36) Grabel'nykh, V. A.; Sukhomazova, E. N.; Levanova, E. P.; Vshivtsev, V. Yu.; Zhanchipova, E. R.; Klyba, L. V.; Albanov, A. I.; Russavskaya, N. V.; Korchevin, N. A. *Russ. J. Gen. Chem.* **2007**, *77*, 1817.

(37) Levason, W.; McAuliffe, C. A.; Murray, S. G. *J. Chem. Soc., Dalton Trans.* **1976**, *3*, 269.

(31) Song, L.-C.; Ge, J.-H.; Liu, X.-F.; Zhao, L.-Q.; Hu, Q.-M. *J. Organomet. Chem.* **2006**, *691*, 5701.

(32) (a) Capon, J.-F.; Gloaguen, F.; Schollhammer, P.; Talarmin, J. *Coord. Chem. Rev.* **2005**, *249*, 1664. (b) Capon, J.-F.; Gloaguen, F.; Pétilion, F. Y.; Schollhammer, P.; Talarmin, J. *Coord. Chem. Rev.* **2009**, *253*, 1476.

ventilated hood, and then the mixture was extracted with  $\text{CHCl}_3$  (30 mL  $\times$  3). After  $\text{CHCl}_3$  was removed, the remaining red oil was distilled under vacuum to give the product as a light yellow oil (0.479 g, 55%), bp 45–46 °C (1 mmHg). This compound was identified by comparison of its IR and  $^1\text{H}$  NMR data with those of an authentic sample prepared by another method.<sup>36</sup>

**Preparation of  $[(\mu\text{-SeCH}_2)_2\text{CH}(\text{OH})]\text{Fe}_2(\text{CO})_6$  (A).** To a deep green solution of  $\text{Fe}_3(\text{CO})_{12}$  (0.504 g, 1.00 mmol) in toluene (25 mL) was added 2-hydroxypropane-1,3-diselenol (0.220 g, 1.00 mmol). The mixture was refluxed for 1.5 h, resulting in a color change from deep green to dark red. After solvent was removed in vacuo, the residue was subjected to flash column chromatography using petroleum ether to remove the soluble and insoluble impurities and then using acetone to elute the major red band. After acetone was removed in vacuo, the residue was further subjected to TLC separation using acetone/petroleum ether (1:4 v/v) as eluent. From the main red band, **A** was obtained as a red solid (0.253 g, 51%), mp 96–97 °C. Anal. Calcd for  $\text{C}_9\text{H}_6\text{Fe}_2\text{O}_7\text{Se}_2$ : C, 21.80; H, 1.22. Found: C, 21.75; H, 1.24. IR (KBr disk):  $\nu_{\text{C}=\text{O}}$  2068 (s), 2024 (vs), 1989 (vs);  $\nu_{\text{O}-\text{H}}$  3418 (m)  $\text{cm}^{-1}$ .  $^1\text{H}$  NMR (300 MHz,  $\text{CDCl}_3$ , TMS): 1.53 (t, 2 $\text{H}_a$ ,  $J_{\text{HaHe}} = J_{\text{HaHa}'} = 11.1$  Hz), 1.85 (d, 1H,  $J = 5.1$  Hz, OH), 2.84 (d, 2 $\text{H}_e$ ,  $J_{\text{HeHa}} = 12.0$  Hz), 2.97–3.03 (m, 1 $\text{H}_a$ ) ppm ( $\text{H}_a$  and  $\text{H}_e$  denote the axially and equatorially bonded H atoms in  $\text{CH}_2\text{Se}$  groups, while  $\text{H}_a'$  and  $\text{H}_e'$  represent those axially or equatorially bonded to bridgehead C atom).  $^{77}\text{Se}$  NMR (57 MHz,  $\text{CDCl}_3$ ,  $\text{Me}_2\text{Se}$ ): 207.36 (s) ppm.

**Preparation of A and  $(\mu\text{-EtSe})[\mu\text{-SeCH}_2\text{CH}(\text{OH})(\text{CH}_2\text{Br})]\text{Fe}_2(\text{CO})_6$  (B).** (i) The procedure for complex **A** as major product: A purple-red solution of  $(\mu\text{-Se}_2)\text{Fe}_2(\text{CO})_6$  (0.438 g, 1.00 mmol) in THF (25 mL) was cooled to –78 °C, and then  $\text{Et}_3\text{BHLi}$  (2.0 mL, 2.00 mmol) was added. The mixture was stirred at –78 °C for 20 min to give a brown-red solution containing  $(\mu\text{-LiSe})_2\text{Fe}_2(\text{CO})_6$ . After 1,3-dibromo-2-propanol (0.12 mL, 1.00 mmol) was added, the new mixture was warmed to room temperature and stirred at this temperature for 12 h. Volatiles were removed in vacuo, and the residue was subjected to TLC separation using  $\text{CH}_2\text{Cl}_2$ /petroleum ether (1:1 v/v) as eluent. From the main red band, **B** was obtained as a red oil (0.080 g, 13%). When the eluent was changed to acetone/petroleum ether (1:4 v/v), **A** was obtained from another main red band as a red solid (0.111 g, 22%). Complex **A** was identified by melting point and IR and  $^1\text{H}$  NMR spectral comparison with the same compound prepared in the reaction of  $(\text{HSeCH}_2)_2\text{CHOH}$  with  $\text{Fe}_3(\text{CO})_{12}$ . Complex **B** was characterized by elemental analysis and spectroscopy. Anal. Calcd for  $\text{C}_{11}\text{H}_{11}\text{BrFe}_2\text{O}_7\text{Se}_2$ : C, 21.85; H, 1.83. Found: C, 22.01; H, 1.85. IR (KBr disk):  $\nu_{\text{C}=\text{O}}$  2064 (s), 2023 (vs), 1980 (vs);  $\nu_{\text{O}-\text{H}}$  3407 (m)  $\text{cm}^{-1}$ .  $^1\text{H}$  NMR (400 MHz,  $d_6$ -acetone, TMS): 1.19 (t,  $J = 7.6$  Hz, a- $\text{CH}_2\text{CH}_3$ ), 1.44 (t,  $J = 7.6$  Hz, e- $\text{CH}_2\text{CH}_3$ ), 1.49 (t,  $J = 7.4$  Hz, e- $\text{CH}_2\text{CH}_3$ ), 2.42–3.07 (m, 4H,  $\text{SeCH}_2\text{CH}_3$ ,  $\text{SeCH}_2\text{CH}$ ), 3.45–3.64 (m, 2H,  $\text{BrCH}_2$ ), 3.74–3.81 (m, e- $\text{CH}_2\text{-CH}$ ), 4.00–4.08 (m, e- $\text{CH}_2\text{CH}$ ), 4.10–4.15 (m, a- $\text{CH}_2\text{CH}$ ), 4.80 (d,  $J = 5.2$  Hz, e- $\text{CH}_2\text{CHOH}$ ), 4.99 (d,  $J = 5.2$  Hz, e- $\text{CH}_2\text{CHOH}$ ), 5.03 (d,  $J = 5.2$  Hz, a- $\text{CH}_2\text{CHOH}$ ) ppm.  $^{77}\text{Se}$  NMR (76 MHz,  $\text{CDCl}_3$ ,  $\text{Me}_2\text{Se}$ ): 95.73 (s), 146.92 (s), 155.84 (s), 160.81 (s), 203.07 (s), 206.97 (s) ppm. (ii) Another procedure for complex **B** as major product: To the prepared THF solution from  $(\mu\text{-Se}_2)\text{Fe}_2(\text{CO})_6$  (0.438 g, 1.00 mmol) and  $\text{Et}_3\text{BHLi}$  (2.0 mL, 2.00 mmol) as described in procedure (i) was added an excess amount 1,3-dibromo-2-propanol (0.36 mL, 3.00 mmol), and then the new mixture was stirred at room temperature for 12 h. After the same workup as that described in procedure (i), complexes **B** (0.190 g, 31%) and **A** (0.015 g, 3.0%) were obtained, respectively.

**Preparation of  $[(\mu\text{-SeCH}_2)_2\text{CH}(\text{OH})]\text{Fe}_2(\text{CO})_5(\text{PPh}_3)$  (1).** A solution of **A** (0.248 g, 0.50 mmol),  $\text{PPh}_3$  (0.131 g, 0.50 mmol), and  $\text{Me}_3\text{NO} \cdot 2\text{H}_2\text{O}$  (0.056 g, 0.50 mmol) in MeCN (15 mL) was stirred at room temperature for 0.5 h. The resulting dark red solution was evaporated to dryness in vacuo, and the residue was separated by TLC using acetone/petroleum ether (1:3.5 v/v) as eluent. From the main red band, **1** was obtained as a red solid (0.295 g, 81%), mp 150 °C (dec). Anal. Calcd for  $\text{C}_{26}\text{H}_{21}$ -

$\text{Fe}_2\text{O}_6\text{PSe}_2$ : C, 42.78; H, 2.90. Found: C, 42.72; H, 2.98. IR (KBr disk):  $\nu_{\text{C}=\text{O}}$  2037 (vs), 1975 (vs), 1928 (m);  $\nu_{\text{O}-\text{H}}$  3387 (m)  $\text{cm}^{-1}$ .  $^1\text{H}$  NMR (400 MHz,  $\text{CDCl}_3$ , TMS): 1.16 (d, 1H,  $J = 3.6$  Hz, OH), 1.27 (d, 2 $\text{H}_a$ ,  $J_{\text{HaHe}} = 11.2$  Hz), 1.54–1.59 (m, 1 $\text{H}_a$ ), 2.23 (d, 2 $\text{H}_e$ ,  $J_{\text{HeHa}} = 10.0$  Hz), 7.45, 7.64 (2s, 15H,  $3\text{C}_6\text{H}_5$ ) ppm.  $^{31}\text{P}$  NMR (162 MHz,  $\text{CDCl}_3$ , 85%  $\text{H}_3\text{PO}_4$ ): 67.88 (s) ppm.  $^{77}\text{Se}$  NMR (57 MHz,  $\text{CDCl}_3$ ,  $\text{Me}_2\text{Se}$ ): 182.38 (s) ppm.

**Preparation of  $[(\mu\text{-SeCH}_2)_2\text{CH}(\text{OCOPh})]\text{Fe}_2(\text{CO})_5(\text{PPh}_3)$  (2).** A solution of **1** (0.365 g, 0.50 mmol) in  $\text{CH}_2\text{Cl}_2$  (15 mL) was cooled to 0 °C, and then  $\text{Et}_3\text{N}$  (0.07 mL, 0.50 mmol) and benzoyl chloride (0.06 mL, 0.50 mmol) were added. The mixture was warmed to room temperature and stirred at this temperature for 12 h. After solvent was removed in vacuo, the residue was subjected to TLC separation using  $\text{CH}_2\text{Cl}_2$ /petroleum ether (1:3 v/v) as eluent. From the main red band, **2** was obtained as a red solid (0.317 g, 76%), mp 95 °C (dec). Anal. Calcd for  $\text{C}_{33}\text{H}_{25}\text{Fe}_2\text{O}_7\text{PSe}_2$ : C, 47.52; H, 3.02. Found: C, 47.40; H, 3.09. IR (KBr disk):  $\nu_{\text{C}=\text{O}}$  2034 (vs), 1977 (vs), 1959 (vs), 1930 (s);  $\nu_{\text{C}=\text{O}}$  1711 (s)  $\text{cm}^{-1}$ .  $^1\text{H}$  NMR (400 MHz,  $\text{CDCl}_3$ , TMS): 1.52 (t, 2 $\text{H}_a$ ,  $J_{\text{HaHe}} = J_{\text{HaHa}'} = 11.4$  Hz), 2.47 (d, 2 $\text{H}_e$ ,  $J_{\text{HeHa}} = 10.0$  Hz), 3.68–3.74 (m, 1 $\text{H}_a$ ), 7.41–8.08 (m, 20H,  $4\text{C}_6\text{H}_5$ ) ppm.  $^{31}\text{P}$  NMR (162 MHz,  $\text{CDCl}_3$ , 85%  $\text{H}_3\text{PO}_4$ ): 67.30 (s) ppm.  $^{77}\text{Se}$  NMR (57 MHz,  $\text{CDCl}_3$ ,  $\text{Me}_2\text{Se}$ ): 190.35 (s) ppm.

**Preparation of  $[(\mu\text{-SeCH}_2)_2\text{CH}(\text{OPPh}_2)\text{-}\eta^1]\text{Fe}_2(\text{CO})_5$  (3).** To a red solution of **A** (0.248 g, 0.50 mmol) in THF (15 mL) cooled to 0 °C were added  $\text{Et}_3\text{N}$  (0.07 mL, 0.50 mmol) and  $\text{Ph}_2\text{PCL}$  (0.09 mL, 0.50 mmol). After the mixture was stirred at 0 °C for 0.5 h, it was allowed to warm to room temperature and stirred at this temperature for 12 h. Solvent was removed in vacuo, and the residue was subjected to TLC separation using  $\text{CH}_2\text{Cl}_2$ /petroleum ether (1:2 v/v) as eluent. From the main red band, **3** was obtained as a red solid (0.255 g, 78%), mp 174 °C (dec). Anal. Calcd for  $\text{C}_{20}\text{H}_{15}\text{Fe}_2\text{O}_6\text{PSe}_2$ : C, 36.85; H, 2.32. Found: C, 36.93; H, 2.27. IR (KBr disk):  $\nu_{\text{C}=\text{O}}$  2043 (s), 1982 (vs), 1963 (vs), 1925 (s)  $\text{cm}^{-1}$ .  $^1\text{H}$  NMR (300 MHz,  $\text{CDCl}_3$ , TMS): 1.97 (d, 2 $\text{H}_a$ ,  $J_{\text{HaHe}} = 12.3$  Hz), 2.60 (d, 2 $\text{H}_e$ ,  $J_{\text{HeHa}} = 9.9$  Hz), 4.39–4.48 (m, 1 $\text{H}_e$ ), 7.48–7.75 (m, 10H,  $2\text{C}_6\text{H}_5$ ) ppm.  $^{31}\text{P}$  NMR (121 MHz,  $\text{CDCl}_3$ , 85%  $\text{H}_3\text{PO}_4$ ): 159.47 (s) ppm.  $^{77}\text{Se}$  NMR (57 MHz,  $\text{CDCl}_3$ ,  $\text{Me}_2\text{Se}$ ): 4.35 (s) ppm.

**Preparation of  $[(\mu\text{-SeCH}_2)_2\text{CH}(\text{OPPhCl})\text{-}\eta^1]\text{Fe}_2(\text{CO})_5$  (4).** To a red solution of **A** (0.248 g, 0.50 mmol) in MeCN (15 mL) was added  $\text{PhPCL}_2$  (0.07 mL, 0.50 mmol), and then the mixture was stirred at room temperature for 12 h. After solvent was removed in vacuo, the residue was subjected to TLC separation using  $\text{CH}_2\text{Cl}_2$ /petroleum ether (1:3 v/v) as eluent. From the main red band, **4** was obtained as a red solid (0.210 g, 69%), mp 143 °C (dec). Anal. Calcd for  $\text{C}_{14}\text{H}_{10}\text{ClFe}_2\text{O}_6\text{PSe}_2$ : C, 27.55; H, 1.65. Found: C, 27.54; H, 1.63. IR (KBr disk):  $\nu_{\text{C}=\text{O}}$  2036 (vs), 1987 (vs), 1970 (vs), 1941 (s)  $\text{cm}^{-1}$ .  $^1\text{H}$  NMR (400 MHz,  $\text{CDCl}_3$ , TMS): 1.95, 2.15 (2d, 2 $\text{H}_a$ ,  $J_{\text{HaHe}} = 12.8$  Hz), 2.54, 2.95 (2d, 2 $\text{H}_e$ ,  $J_{\text{HeHa}} = 12.8$  Hz), 4.62–4.66 (m, 1 $\text{H}_e$ ), 7.60–8.02 (m, 5H,  $\text{C}_6\text{H}_5$ ) ppm.  $^{31}\text{P}$  NMR (162 MHz,  $\text{CDCl}_3$ , 85%  $\text{H}_3\text{PO}_4$ ): 207.66 (s) ppm.  $^{77}\text{Se}$  NMR (57 MHz,  $\text{CDCl}_3$ ,  $\text{Me}_2\text{Se}$ ): 10.98 (s), 43.03 (s) ppm.

**Preparation of  $(\mu\text{-EtSe})[\mu\text{-SeCH}_2\text{CH}(\text{CH}_2\text{Br})(\text{O}_2\text{CC}_5\text{H}_4\text{N-4})]\text{Fe}_2(\text{CO})_6$  (5).** A solution of **B** (0.302 g, 0.50 mmol) in  $\text{CH}_2\text{Cl}_2$  (15 mL) was cooled to 0 °C, and then  $\text{Et}_3\text{N}$  (0.07 mL, 0.50 mmol) and 4-pyridinecarboxylic acid chloride (0.071 g, 0.50 mmol) were added. After the mixture was stirred at 0 °C for 0.5 h, it was warmed to room temperature and stirred at this temperature for 12 h. Solvent was removed in vacuo, and the residue was subjected to TLC separation using  $\text{CH}_2\text{Cl}_2$  as eluent. From the main orange-red band, **5** was obtained as a red oil (0.352 g, 99%). Anal. Calcd for  $\text{C}_{17}\text{H}_{14}\text{BrFe}_2\text{NO}_8\text{Se}_2$ : C, 28.77; H, 1.99; N, 1.97. Found: C, 28.67; H, 2.07; N, 2.08. IR (KBr disk):  $\nu_{\text{C}=\text{O}}$  2064 (s), 2025 (vs), 1982 (vs);  $\nu_{\text{C}=\text{O}}$  1737 (s)  $\text{cm}^{-1}$ .  $^1\text{H}$  NMR (300 MHz,  $\text{CDCl}_3$ , TMS): 1.13 (t,  $J = 7.5$  Hz, a- $\text{CH}_2\text{CH}_3$ ), 1.38 (t,  $J = 7.5$  Hz, e- $\text{CH}_2\text{CH}_3$ ), 1.45 (t,  $J = 7.5$  Hz, e- $\text{CH}_2\text{CH}_3$ ), 2.22–3.07 (m, 4H,  $\text{SeCH}_2\text{CH}_3$ ,  $\text{SeCH}_2\text{CH}$ ), 3.63–3.71 (m, 2H,  $\text{BrCH}_2$ ), 5.03–5.10 (m, e- $\text{CH}_2\text{CH}$ ), 5.37–5.44 (m, e- $\text{CH}_2\text{CH}$ ), 5.49–5.55 (m, a- $\text{CH}_2\text{CH}$ ), 7.95 (s, 2H, 2  $\alpha$ -H of pyridine ring), 9.00 (s, 2H, 2  $\beta$ -H of pyridine

**Table 4. Crystal Data and Structure Refinements for A, 1, and 2**

	A	1	2
mol formula	C <sub>9</sub> H <sub>6</sub> Fe <sub>2</sub> O <sub>6</sub> Se <sub>2</sub>	C <sub>26</sub> H <sub>21</sub> Fe <sub>2</sub> O <sub>6</sub> PSe <sub>2</sub>	C <sub>33</sub> H <sub>25</sub> Fe <sub>2</sub> O <sub>7</sub> P Se <sub>2</sub> ·CHCl <sub>3</sub>
mol wt	495.76	730.02	953.49
cryst syst	orthorhombic	monoclinic	triclinic
space group	<i>Pbca</i>	<i>P2<sub>1</sub>/c</i>	<i>P</i> $\bar{1}$
<i>a</i> /Å	13.699(3)	9.2439(18)	10.3184(8)
<i>b</i> /Å	21.795(4)	17.764(4)	15.9031(11)
<i>c</i> /Å	29.394(6)	16.640(3)	22.649(2)
$\alpha$ /deg	90	90	99.005(10)
$\beta$ /deg	90	102.25(3)	90.353(12)
$\gamma$ /deg	90	90	94.881(8)
<i>V</i> /Å <sup>3</sup>	8777(3)	2670.2(9)	3656.8(5)
<i>Z</i>	24	4	4
<i>D<sub>c</sub></i> /g·cm <sup>-3</sup>	2.251	1.816	1.732
abs coeff/mm <sup>-1</sup>	6.982	3.912	3.093
<i>F</i> (000)	5664	1440	1888
index ranges	-17 ≤ <i>h</i> ≤ 17 -27 ≤ <i>k</i> ≤ 27 -26 ≤ <i>l</i> ≤ 37	-11 ≤ <i>h</i> ≤ 10 -21 ≤ <i>k</i> ≤ 15 -19 ≤ <i>l</i> ≤ 18	-13 ≤ <i>h</i> ≤ 13 -20 ≤ <i>k</i> ≤ 20 -29 ≤ <i>l</i> ≤ 26
no. of reflns	58 306	17 942	31 100
no. of indep reflns	9715	4705	17 118
2 $\theta$ <sub>max</sub> /deg	54.30	50.04	55.74
<i>R</i>	0.0372	0.0376	0.0568
<i>R<sub>w</sub></i>	0.0798	0.0726	0.1040
goodness of fit	1.046	0.978	1.048
largest diff peak and hole/e Å <sup>-3</sup>	0.612/-0.797	0.555/-0.798	0.789/-0.609

ring) ppm. <sup>77</sup>Se NMR (76 MHz, CDCl<sub>3</sub>, Me<sub>2</sub>Se): 86.93 (s), 136.05 (s), 151.95 (s), 154.46 (s), 199.79 (s), 203.59 (s) ppm.

**Preparation of (μ-EtSe)[μ-SeCH<sub>2</sub>CH(CH<sub>2</sub>Br)(OPPh<sub>2</sub>-η<sup>1</sup>)]Fe<sub>2</sub>(CO)<sub>5</sub> (6).** A solution of **B** (0.302 g, 0.50 mmol) in THF (15 mL) was cooled to 0 °C, and then Et<sub>3</sub>N (0.07 mL, 0.50 mmol) and Ph<sub>2</sub>PCl (0.09 mL, 0.50 mmol) were added. The mixture was stirred at 0 °C for 0.5 h, and then the mixture was warmed to room temperature and stirred at this temperature for 12 h. After removal of solvent, the residue was subjected to TLC separation using CH<sub>2</sub>Cl<sub>2</sub>/petroleum ether (1:3 v/v) as eluent. From the main red band, **6** was obtained as a red solid (0.152 g, 40%), mp 154 °C (dec). Anal. Calcd for C<sub>22</sub>H<sub>20</sub>BrFe<sub>2</sub>O<sub>6</sub>PSe<sub>2</sub>: C, 34.73; H, 2.65. Found: C, 34.75; H, 2.59. IR (KBr disk): ν<sub>C=O</sub> 2036 (vs), 1977 (vs), 1960 (vs), 1919 (s) cm<sup>-1</sup>. <sup>1</sup>H NMR (300 MHz, CDCl<sub>3</sub>, TMS): 0.96 (t, 3H, *J* = 7.0 Hz, CH<sub>3</sub>), 1.93–2.39 (m, 4H, e-CH<sub>2</sub>CH<sub>3</sub>, a-CH<sub>2</sub>CH), 3.36 (br s, 2H, a-CH<sub>2</sub>CHCH<sub>2</sub>Br), 3.57–3.63 (m, 1H, a-CH<sub>2</sub>CH), 7.40–7.93 (m, 10H, 2C<sub>6</sub>H<sub>5</sub>) ppm. <sup>31</sup>P NMR (121 MHz, CDCl<sub>3</sub>, 85% H<sub>3</sub>PO<sub>4</sub>): 171.12 (s) ppm. <sup>77</sup>Se NMR (57 MHz, CDCl<sub>3</sub>, Me<sub>2</sub>Se): 110.32 (s), 192.58 (s) ppm.

**X-ray Structure Determinations of A, 1–4, and 6.** Single crystals of **A**, **1–4**, and **6** suitable for X-ray diffraction analysis were grown by slow evaporation of the CHCl<sub>3</sub>/petroleum ether solutions of **A** and **2** or the CH<sub>2</sub>Cl<sub>2</sub>/petroleum ether solutions of **1**, **3**, **4**, and **6** at about -4 °C. Each crystal was mounted on a Rigaku MM-007 (rotating anode) diffractometer equipped with Saturn 70CCD. Data were collected at room temperature, using a confocal monochromator with Mo K $\alpha$  radiation ( $\lambda$  = 0.71070 Å) in the  $\omega$ - $\phi$  scanning mode. Data collection, reduction, and absorption correction were performed by the CRYSTAL-CLEAR program.<sup>38</sup> The structures were solved by direct methods using the SHELXS-97 program<sup>39</sup> and refined by full-matrix

(38) Sheldrick, G. M. *SADABS, A Program for Empirical Absorption Correction of Area Detector Data*; University of Göttingen: Germany, 1996.

(39) Sheldrick, G. M. *SHELXS97, A Program for Crystal Structure Solution*; University of Göttingen: Germany, 1997.

**Table 5. Crystal Data and Structure Refinements for 3, 4, and 6**

	3	4	6
mol formula	C <sub>20</sub> H <sub>15</sub> Fe <sub>2</sub> O <sub>6</sub> PSe <sub>2</sub>	C <sub>14</sub> H <sub>10</sub> ClFe <sub>2</sub> O <sub>6</sub> PSe <sub>2</sub>	C <sub>22</sub> H <sub>20</sub> BrFe <sub>2</sub> O <sub>6</sub> PSe <sub>2</sub>
mol wt	651.91	610.26	760.88
cryst syst	monoclinic	monoclinic	triclinic
space group	<i>P2(1)/c</i>	<i>C2/c</i>	<i>P</i> $\bar{1}$
<i>a</i> /Å	12.116(2)	22.423(5)	10.383(5)
<i>b</i> /Å	17.491(4)	7.9680(16)	11.346(5)
<i>c</i> /Å	11.902(2)	23.872(5)	11.524(5)
$\alpha$ /deg	90	90	91.620
$\beta$ /deg	115.13(3)	112.57(3)	98.648(3)
$\gamma$ /deg	90	90	106.563(7)
<i>V</i> /Å <sup>3</sup>	2283.6(8)	3938.5(14)	1282.9(10)
<i>Z</i>	4	8	2
<i>D<sub>c</sub></i> /g·cm <sup>-3</sup>	1.896	2.058	1.970
abs coeff/mm <sup>-1</sup>	4.562	5.413	5.623
<i>F</i> (000)	1272	2352	740
index ranges	-14 ≤ <i>h</i> ≤ 13 -19 ≤ <i>k</i> ≤ 20 -14 ≤ <i>l</i> ≤ 14	-26 ≤ <i>h</i> ≤ 26 -9 ≤ <i>k</i> ≤ 9 -24 ≤ <i>l</i> ≤ 28	-11 ≤ <i>h</i> ≤ 13 -13 ≤ <i>k</i> ≤ 14 -15 ≤ <i>l</i> ≤ 15
no. of reflns	16 798	12 480	9447
no. of indep reflns	3946	3471	6029
2 $\theta$ <sub>max</sub> /deg	50.02	50.04	55.76
<i>R</i>	0.0698	0.0332	0.0424
<i>R<sub>w</sub></i>	0.1624	0.0615	0.1028
goodness of fit	1.033	0.910	0.962
largest diff peak and hole/e Å <sup>-3</sup>	2.072/-1.259	0.548/-0.728	1.207/-1.617

least-squares techniques (SHELXL-97)<sup>40</sup> on *F*<sup>2</sup>. Hydrogen atoms were located by using the geometric method. Details of crystal data, data collections, and structure refinements are summarized in Tables 4 and 5, respectively.

**Electrochemistry.** Acetonitrile (Fisher Chemicals, HPLC grade) was used for performance of electrochemistry. A solution of 0.1 M *n*-Bu<sub>4</sub>NPF<sub>6</sub> in MeCN was used as electrolyte in all cyclic voltammetric experiments. The electrolyte solution was degassed by bubbling with CO for about 10 min before measurement. Electrochemical measurements were made using a BAS Epsilon potentiostat. All voltammograms were obtained in a three-electrode cell with a 3 mm diameter glassy carbon working electrode, a platinum counter electrode, and an Ag/Ag<sup>+</sup> (0.01 M AgNO<sub>3</sub>/0.1 M *n*-Bu<sub>4</sub>NPF<sub>6</sub> in MeCN) reference electrode under CO. The working electrode was polished with 0.05 μm alumina paste and sonicated in water for about 10 min. Bulk electrolysis was run on a vitreous carbon rod (*A* = 2.9 cm<sup>2</sup>) in a two-compartment, gastight, H-type electrolysis cell containing ca. 25 mL of MeCN. Gas chromatography was performed with a Shimadzu GC-2014 gas chromatograph under isothermal conditions with nitrogen as a carrier gas and a thermal conductivity detector.

**Acknowledgment.** We are grateful to the National Natural Science Foundation of China and the Research Fund for the Doctoral Program of Higher Education of China for financial support.

**Supporting Information Available:** Full tables of crystal data, atomic coordinates, thermal parameters, bond lengths and angles for **A**, **1–4**, and **6** as CIF files, and cyclic voltammogram of **C**. This material is available free of charge via the Internet at <http://pubs.acs.org>.

(40) Sheldrick, G. M. *SHELXL97, A Program for Crystal Structure Refinement*; University of Göttingen: Germany, 1997.